Article

2018 Atmospheric Motion Vector (AMV) Intercomparison Study

David Santek[1], Richard Dworak[1], Sharon Nebuda[1], Steve Wanzong[1], Régis Borde[2], Iliana Genkova[3], Javier García-Pereda[4], Renato Galante Negri[5], Manuel Carranza[6], Kenichi Nonaka[7], Kazuki Shimoji[7], Soo Min Oh[8,9], Byung-Il Lee[9], Sung-Rae Chung[9], Jaime Daniels[10], Wayne Bresky[11]

[1] Space Science and Engineering Center (SSEC), University of Wisconsin-Madison, 1225 West Dayton Street, Madison, Wisconsin 53706, United States; dave.santek@ssec.wisc.edu, rdworak@ssec.wisc.edu, sharon.nebuda@ssec.wisc.edu, steve.wanzong@ssec.wisc.edu

[2] EUMETSAT, Eumetsat Allee 1, 64295 Darmstadt, Germany; regis.borde@eumetsat.int

[3] I.M. Systems Group at National Centers for Environmental Prediction (NCEP), National Oceanic and Atmospheric Administration (NOAA), 5830 University Research Court, College Park, Maryland 20740, United States; iliana.genkova@noaa.gov

[4] Satellite Application Facility on support to Nowcasting (NWCSAF), Agencia Estatal de Meteorología (AEMET), Leonardo Prieto Castro 8, 28040 Madrid, Spain; jgarciap@aemet.es

[5] Center for Weather Prediction and Climate Studies (CPTEC), National Institute for Space Research (INPE), 12630-000 Cachoeira Paulista, São Paulo, Brazil; renato.galante@inpe.br

[6] GMV INSYEN at EUMETSAT, Eumetsat Allee 1, 64295 Darmstadt, Germany; manuel.carranza@external.eumetsat.int

[7] Japan Meteorological Agency, 1-3-4 Otemachi, Chiyoda-ku, Tokyo 100-8122, Japan; k-nonaka@met.kishou.go.jp, kazuki.shimoji@met.kishou.go.jp

[8] Department of Physics and Astronomy, Seoul National University, 1, Gwanak-ro, Gwanak-gu, Seoul 08826, Republic of Korea; dotoa@snu.ac.kr

[9] National Meteorological Satellite Center (NMSC), Korea Meterological Administration (KMA), 64-18, Guam-gil, Gwanghyewon-myeon, Jincheon-gun, Chungcheongbuk-do 27803, Republic of Korea; bilee01@korea.kr, csr@korea.kr

[10] Center for Satellite Applications and Research (STAR), National Environmental Satellite, Data and Information Service (NESDIS), National Oceanic and Atmospheric Administration (NOAA), 5830 University Research Court, College Park, Maryland 20740, United States; jaime.daniels@noaa.gov

[11] I.M. Systems Group at Center for Satellite Applications and Research (STAR), National Environmental Satellite, Data and Information Service (NESDIS), National Oceanic and Atmospheric Administration (NOAA), 5830 University Research Court, College Park, Maryland 20740, United States; wayne.bresky@noaa.gov

Abstract:

Atmospheric Motion Vectors (AMVs) calculated by six different institutions (Brazil Center for Weather Prediction and Climate Studies/CPTEC/INPE, European Organization for the Exploitation of Meteorological Satellites/EUMETSAT, Japan Meteorological Agency/JMA, Korea Meteorological Administration/KMA, Unites States National Oceanic and Atmospheric Administration/NOAA and the Satellite Application Facility on Support to Nowcasting/NWCSAF) with JMA's Himawari-8 satellite data and other common input data are here compared. The comparison is based on two different AMV input datasets, calculated with two different image triplets for 21 July 2016, and the use of a prescribed and a specific configuration.

The main results of the study are summarized as follows: (1) the differences in the AMV datasets depend very much on the "AMV height assignment" used and much less on the use of a prescribed or specific configuration; (2) the use of the "Common Quality Indicator (CQI)" has a quantified skill in filtering collocated AMVs for an improved statistical agreement between centers; (3) JMA AMV algorithm has the best overall performance considering all validation metrics, most likely due to its height assignment: "optimal estimation using observed radiance and NWP wind vertical profile".

Keywords: Atmospheric Motion Vectors (AMVs); Intercomparison; Himawari; CPTEC/INPE; EUMETSAT; JMA; KMA; NOAA; NWCSAF.

Peer-reviewed version available at Remote Sens. 2019, 11, 2240; doi:10.3390/rs11192240

1. Introduction

The use of satellite-derived cloud displacements to infer atmospheric motion (AMVs or Atmospheric Motion Vectors) has been investigated since the first weather satellites were launched. In the early 1960s, Tetsuya Fujita developed analysis techniques to use cloud pictures from the first Television Infrared Observation Satellite (TIROS), a polar orbiter, for estimating the velocity of tropospheric winds [1]. Throughout the 1970s and early 1980s, AMVs were produced from geostationary satellite data using a combination of automated and manual techniques.

The following is a brief chronology on the generation of AMVs from the primary producers:

- In 1969, the NOAA National Environmental Satellite Service (NESS, now NESDIS), began routine production of a completely manual technique for producing wind vectors from viewing time loops of visible satellite images, resulting in approximately 300 AMVs per day [2]. The technique was partially computerized in the 1970s, automated in the 1990s, and was recently updated for the GOES-R series satellites [3].
- The University of Wisconsin-Madison (UW) Space Science and Engineering Center (SSEC) developed a computerized algorithm to manually track clouds from imagery of the first generation of geostationary weather satellites [4]. This technique was fully automated in the 1990s [5], and variations of this technique are still in use today.
- The extraction of AMVs from Meteosat infrared imagery has been operational at the European Space Operations Centre (ESOC) and EUMETSAT since the late 1970s. After several major improvements, the extraction technique reached a stage in 1991 where the majority of the vectors represented the local wind field [6]. The algorithm has been updated in 2012 including the CCC method to set the AMV altitude [7].
- The Geostationary Meteorological Satellite (GMS) was launched on July 1977 as the first Japanese geostationary meteorological satellite, and operated from 1978 to 1984. The Japan Meteorological Agency/Meteorological Satellite Center (JMA/MSC) routinely began AMV derivation provided twice a day from the GMS satellite imagery in 1978, by using the Cloud Wind Estimation System (CWES) [8]. The derivation system was fully automated in 2003, and AMVs are today calculated every hour by the latest algorithm adapted to Himawari-8.
- Atmospheric Motion Vectors have been produced operationally at Brazil Center for Weather Prediction and Climate Studies (CPTEC/INPE) since 1998. The original algorithm was based in the routines developed by ESOC, and adapted to use GOES-8 10.8 μm infrared images [9]. AMVs from the water vapour channel were added to the operational suite, followed by the 3.9 μm and visible channels in 2006 to estimate winds from lower troposphere only [10]. More recently, the algorithm has been adapted to data from GOES-16.
- The Korea Meteorological Administration (KMA) developed an AMV algorithm for COMS satellite since 2003. Now it is in charge of the AMV algorithm for GEO-KOMPSAT-2 satellites [11].
- The EUMETSAT NWCSAF delivered the first version of its AMV product "HRW/High Resolution Winds" for MSG satellites, inside the 2004 release of its software package

"NWC/MSG". A major change occurred in 2011, with the inclusion of "CCC method" for the AMV height assignment [7]. Progressive extensions have also permitted to calculate AMVs with additional geostationary satellite series all throughout the world (GOES-N in 2016, Himawari-8/9 in 2018, and GOES-R expected in 2019) [12].

However, it was not until 2008 that a coordinated effort was organized to compare the AMVs from the primary AMV producing centres. Overall, this resulted in a total of three "Atmospheric Motion Vector (AMV) Intercomparison studies", which took place over the last decade: Genkova et al. 2008 & 2010 [13, 14], and Santek et al. 2014 [15]. The studies assessed how satellite-derived cloudy AMVs compared in terms of coverage, speed, direction, and cloud height.

The algorithms used for the AMV calculation, and the geostationary satellites with which this process is done, have evolved very much since then, with a new generation of satellites with additional spectral channels bearing new information on cloud microphysics, and with a higher temporal resolution which allows a better understanding of the characteristics of the tracked features.

All this has defined the need for a new "AMV Intercomparison study" in 2018, and the need to formally publish for the first time the results of these Intercomparisons. The study will act as an input for the development of all AMV algorithms, for their optimal use with this new generation of geostationary satellites.

Three main goals are considered for this study:

1) To verify the advantages of the calculation of AMVs with the new generation of geostationary satellites that began with Himawari-8, with better spatial and temporal resolution and new spectral channels, with respect to those calculated with previous satellite series like MSG (Meteosat Second Generation).
2) To compute a "Common Quality Indicator (CQI)" for all centers, based on the "EUMETSAT Quality Indicator" [16], to verify if there is a better agreement between the different AMV datasets.
3) To extract conclusions about the best options for the calculation of AMVs with this new generation of geostationary satellites, considering the options taken by the different centers for their AMV calculation.

Peer-reviewed version available at Remote Sens. 2019, 11, 2240; doi:10.3390/rs11192240

2. Materials and Methods

The geostationary AMV algorithms defined by the following six AMV producers are analyzed here. The three-letter abbreviations are used as identifiers of the AMV datasets throughout the remainder of this article:

BRZ: Brazil Center for Weather Prediction and Climate Studies (CPTEC/INPE)
EUM: European Organization for the Exploitation of Meteorological Satellites (EUMETSAT)
JMA: Japan Meteorological Agency
KMA: Korea Meteorological Administration
NOA: United States National Oceanic and Atmospheric Administration (NOAA)
NWC: Satellite Application Facility on Support to Nowcasting (NWCSAF)

Full information on the AMV algorithms used here can be obtained from the "Operational AMV Product Survey", available at the "International Winds Working Group (IWWG)" webpage [17]. Considering a short summary of these characteristics:

- All algorithms are operational at the corresponding centers, although some of them not with Himawari satellites (BRZ, EUM and NOA).
- Most products are distributed through the GTS while some are produced locally (NWC).
- Many output formats are available, although all AMV algorithms include the heritage Binary Universal Form for the Representation of meteorological data (BUFR) sequence, and most of them have plans of implementing the 2018 new BUFR sequence (3.10.077) for AMVs.
- There is an important variability in the way NWP data and other input products are used by the different AMV algorithms, and also in the way the AMV features are defined.
- Square features of different sizes between 7x7 pixels and 31x31 pixels are used for the processing by the different AMV algorithms. The square features are located in a regular grid with a nominal spacing of 12 km to 72 km, although some methods infer corrections to optimize the location of each feature.
- "Cross Correlation method" is used for the AMV tracking by all centers except NOA, which uses the "Sum of Squared Differences". The "Cross correlation threshold" and the way the tracking is implemented is slightly different for each algorithm.
- All algorithms except BRZ calculate for the study the AMV displacement as the average of two intermediate components; EUM and NOA additionally use the central image of each triplet as reference and tracks backward for the first intermediate component and then forward for the second intermediate component.
- There is an important variability in the height assignment method used by the different centers. For example "Cross correlation contribution (CCC)" is used by EUM and NWC; "Effective black body temperature (EBBT)" with optional WV/IR ratioing and CO_2 slicing corrections are used by BRZ and KMA; an "Optimal estimation method" considering the observed IR radiances, the vertical profile of the NWP wind and the estimated brightness temperature using a radiative transfer model is used by JMA. Some thresholds and corrections are additionally implemented by each center for its specific implementation.

- The "Quality indicator without forecast" (using a specific implementation), and the "Common quality indicator without forecast" (using a common implementation and code) are implemented by all AMV algorithms. The "Quality indicator with forecast" (using a specific implementation) is implemented by all AMV algorithms except BRZ.
- The "Quality indicator threshold" and several other quality checks are different for each algorithm. Additionally, other quality methods are included by some centers: the "Expected Error" (KMA and NOA) and the "Orographic flag" (NWC).

The AMV outputs were originated at the different participating centers considering the following input data:

- Two triplets of Himawari-8/AHI infrared 10.4 μm full–disk images for 21 July 2016 at 0530-0550 UTC and 1200-1220 UTC, one of which images is shown in **Figure 1**. Information was provided at each Himawari-8 pixel for the following variables: latitude, longitude, scanning time, satellite and solar zenith angles, radiance and brightness temperature.
- Auxiliary files containing land/sea mask, land cover and elevation for each Himawari-8 pixel.
- ECMWF ERA-Interim NWP analysis [18] for the given day, for 37 vertical levels every 6 hours, on a regular latitude/longitude grid with a resolution of 0.5°. Information was provided for the following variables: geopotential, surface pressure, temperature, dew point temperature, 2m temperature, skin temperature, relative humidity, wind components, 10m wind components, ozone mixing ratio, total column ozone, land/sea mask, sea/ice cover, snow depth and mean sea level pressure.
- Cloud products derived by NOAA/NESDIS for the given time slots. Information was provided for the following variables: surface type, surface elevation, land class, cloud probability, cloud mask, cloud type, cloud phase and cloud top pressure. However, due to the different cloud assignment methods and the way cloud data are used in them by the different AMV algorithms, only EUM, NOA and NWC made an actual use of these NOAA/NESDIS cloud products.

The image data are equivalent to those used by the "International Cloud Working Group (ICWG)" for the "Cloud Intercomparison study", to improve synergies between both studies. The day was selected due to the variability of meteorological features found in the different regions.

The AMV outputs provided by each AMV algorithm, are analyzed in three independent experiments, designed to measure differences related to specific aspects of the algorithms. Software tools used in the three previous intercomparison studies (Genkova et al. 2008 & 2010 [13, 14], and Santek et al. 2014 [15]) have been used again, so allowing for the comparison of the results in the different studies.

The AMV datasets produced by the different producers for the AMV Intercomparison, and all software tools used throughout the Intercomparison for the verification of the AMV datasets, have been made available such as described in the "Supplementary Materials" chapter.

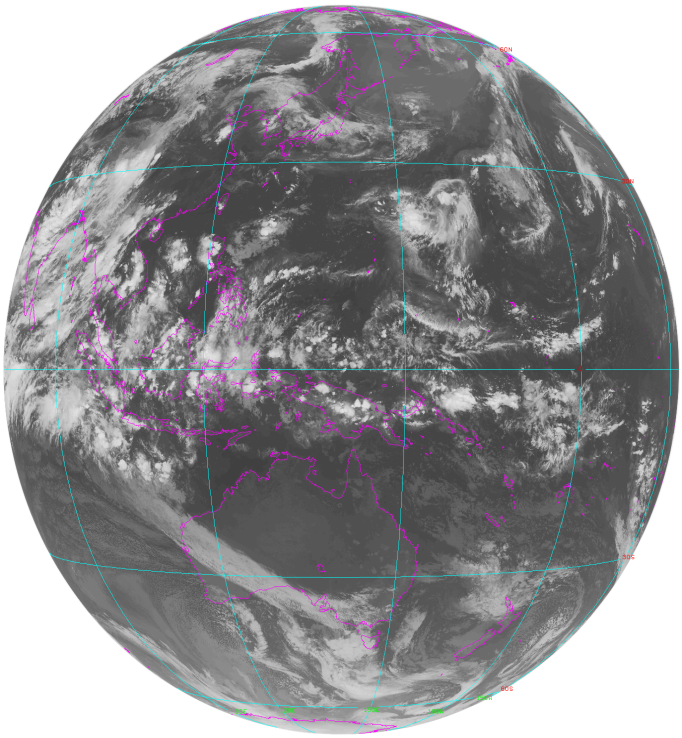

Figure 1. Himawari-8 10.4 μm satellite image for 21 July 2016 at 1200 UTC.

The AMV output from each center for the considered experiments in this Intercomparison study included data for the following variables shown in **Table 1.**

Table 1. Reported variables

Parameter	Code	Description
1	IDN	AMV Identification Number
2	LAT[degrees]	AMV Latitude
3	LON[degrees]	AMV Longitude
4	TS[pixels]	Target Box Size
5	SS[pixels]	Search Box Size
6	SPD[m/s]	AMV Speed
7	DIR[degrees]	AMV Direction (0: due North, 90: due East, 180: due South, 270: due West)
8	PRES[hPa]	AMV Pressure
9	L	Low Level Correction Flag (0: No correction, 1: Inversion correction, 2: Cloud base)
10	NWPSPD[m/s]	Background NWP guess wind speed
11	NWPDIR[degrees]	Background NWP guess wind direction
12	ALB[%]	0.8 μm Albedo at center pixel of target box
13	CORR[%]	Maximum value of Tracking Correlation
14	T	Tracking Method Flag (0: Cross correlation, 1: Sum of squared differences, 2:Other)
15	PRESERR[hPa]	AMV Pressure error
16	H	Height Assignment Method Flag (0: EBBT, 1: CO_2 Slicing, 2: IR/WV ratioing, 3:CCC, 4: Other)
17	QINF[%]	Quality Indicator without forecast
18	QIF[%]	Quality Indicator with forecast
19	CQI[%]	Common Quality Indicator

Peer-reviewed version available at Remote Sens. 2019, 11, 2240; doi:10.3390/rs11192240

3. Results and Discussion

3.1. Experiment 1

In this case, AMV producers extracted cloudy AMVs with the Himawari-8/AHI IR10.4 μm image triplet 1200-1220 UTC, using their best options for the AMV calculation, but with prescribed target box sizes (16x16 pixels), search scene sizes (54x54 pixels) and target locations (with a line and column separation of 16 pixels).

This way, differences in the AMV densities and in all AMV extraction processes (tracer selection, tracer tracking, height assignment and quality control) could be compared, verifying exactly equivalent AMV datasets.

Considering in **Table 2** the parameter distribution for the AMV datasets, with a Common Quality Indicator threshold of 50% (CQI >= 50%):

Table 2. Parameter distribution for Experiment 1 for the different AMV datasets, considering Common Quality Indicator (CQI) >= 50%:

	BRZ	EUM	JMA	KMA	NOA	NWC
Total AMVs	70312	30868	76075	58479	38242	14602
CQI >= 50%	57613	27097	33717	52685	36172	14283
SPD_min (m/s)	2.56	2.51	2.50	2.50	3.00	2.50
SPD_max (m/s)	66.05	139.93	69.97	97.01	92.29	68.77
SPD_mean (m/s)	11.81	13.64	13.29	13.66	14.06	13.64
P_min (hPa)	100.00	57.11	125.00	102.08	102.05	101.00
P_max (hPa)	1000.00	1004.00	994.32	997.66	977.82	965.50
P_mean (hPa)	533.19	437.37	496.89	408.80	432.19	386.40
Low_AMVs (%)	37.10	26.66	31.43	23.05	33.77	23.61
Mid_AMVs (%)	20.33	14.56	19.34	13.29	2.63	8.96
High_AMVs (%)	42.57	58.78	49.23	63.66	63.59	67.43
Low_SPD_min (m/s)	2.56	2.52	2.50	2.50	3.00	2.57
Low_SPD_max (m/s)	35.67	99.02	41.20	70.19	40.52	28.57
Low_SPD_mean (m/s)	9.61	9.33	9.06	9.67	10.21	9.95
Low_P_min (hPa)	700.00	700.23	700.01	700.00	700.06	700.00
Low_P_max (hPa)	1000.00	1004.00	994.32	997.66	977.82	965.50
Low_P_mean (hPa)	874.49	823.71	888.89	820.21	837.59	782.70
Mid_SPD_min (m/s)	2.61	2.53	2.50	2.50	3.06	2.51
Mid_SPD_max (m/s)	66.05	94.60	69.25	70.08	78.86	48.12
Mid_SPD_mean (m/s)	13.61	14.58	14.03	14.53	22.14	17.05
Mid_P_min (hPa)	400.02	400.03	400.01	400.03	400.01	400.05
Mid_P_max (hPa)	699.98	699.77	699.99	699.90	449.96	699.50
Mid_P_mean (hPa)	536.33	531.56	528.20	521.45	425.91	536.54
High_SPD_min (m/s)	2.58	2.51	2.50	2.50	3.00	2.50
High_SPD_max (m/s)	62.47	139.93	69.97	97.01	92.29	68.77
High_SPD_mean (m/s)	12.88	15.37	15.69	14.92	15.77	14.47
High_P_min (hPa)	100.00	57.11	125.00	102.08	102.05	101.00
High_P_max (hPa)	400.00	399.94	399.98	399.97	399.99	400.00
High_P_mean (hPa)	234.17	238.80	234.32	236.29	217.14	227.70

Preprints (www.preprints.org) | NOT PEER-REVIEWED | Posted: 2 August 2019 doi:10.20944/preprints201908.0017.v1

Peer-reviewed version available at Remote Sens. 2019, 11, 2240; doi:10.3390/rs11192240

- The total number of AMVs ranges from 58,000 to 76,000, with lower values for NOA (38,000), EUM (31,000) and NWC (15,000). The number of AMVs is much larger with Himawari satellites than in the previous "AMV Intercomparison" with MSG satellite [15], which found up to approximately 10,000 AMVs. This is due, in part, to the higher resolution of Himawari/AHI (2 km) versus MSG/SEVIRI (3 km), more oceanic regions, and fewer deserts.
- The maximum speed ranges from 66 m s^{-1} (BRZ) to 97 m s^{-1} (KMA), with outliers of 140 m s^{-1} for EUM.
- The minimum pressure is approximately 100 hPa, except for EUM which is at 57 hPa.
- The percentage of AMVs by layer (low layer between 700 and 1000 hPa, medium layer between 400 and 700 hPa, and high layer between 100 and 400 hPa) are respectively 23% to 37%, 9% to 20%, and 43% to 67%. The main outlier of these is NOA at medium levels with only 3%.

Figure 2 shows the spatial localization of AMVs inside the Himawari-8 Full Disk, and the distribution of parameters (Common Quality Indicator, Speed, Direction and Pressure) for the different AMV datasets, considering Common Quality Indicator (CQI) >= 50%:

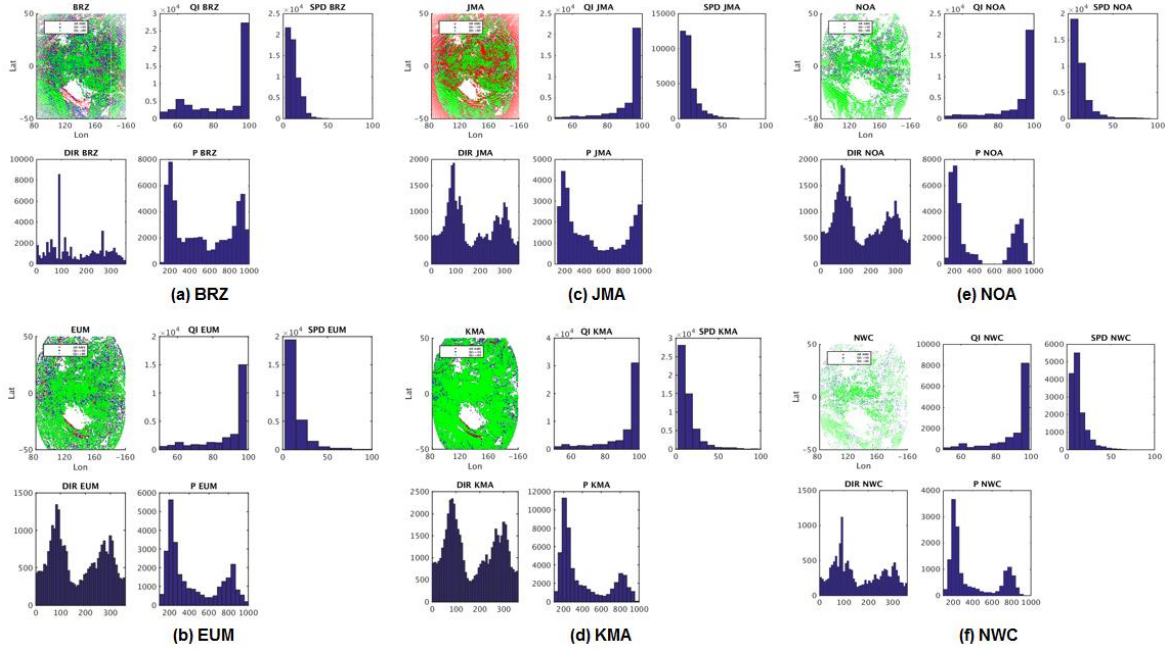

Figure 2. AMV spatial localization and Distribution of parameters for Experiment 1 considering Common Quality Indicator (CQI) >= 50% (Common Quality Indicator, Speed, Direction, Pressure) for the different AMV datasets: (a) BRZ, (b) EUM, (c) JMA, (d) KMA, (e) NOA, (f) NWC.

The distributions are generally similar for all centers, with much better general agreement than in the previous "AMV Intercomparison" [15], but with following items to be taken into account:

1) The distribution of direction values for BRZ shows some directions much more frequent than others, with two anomalous peaks at 90° and 270°. This issue also partially seems to occur with NWC, with a possible anomalous peak at 90°.
2) The distribution of the "Common Quality Indicator (CQI)" values is rather similar for all centers. This circumstance does not happen when the other Quality indicators are considered: "Quality indicator with forecast (QIF)" or "Quality indicator without forecast (QINF)", for which the calculation results are quite different for the different centers (not shown).

Preprints (www.preprints.org) | NOT PEER-REVIEWED | Posted: 2 August 2019 doi:10.20944/preprints201908.0017.v1

Peer-reviewed version available at Remote Sens. 2019, 11, 2240; doi:10.3390/rs11192240

3) The distribution of AMV pressure values is the most divergent for the different centers, due to the different AMV height assignment methods used; only EUM and NWC being similar because of both using "CCC method". This last result is even more evident looking to **Figure 4**, in which the scatter plot of AMV pressures of all centers is shown using the EUM pressure as reference.

Considering in **Figure 3** the parameter plot for different variables for collocated AMVs from the different centers with Common Quality Indicator >= 50%, and a collocation distance up to 55 km:

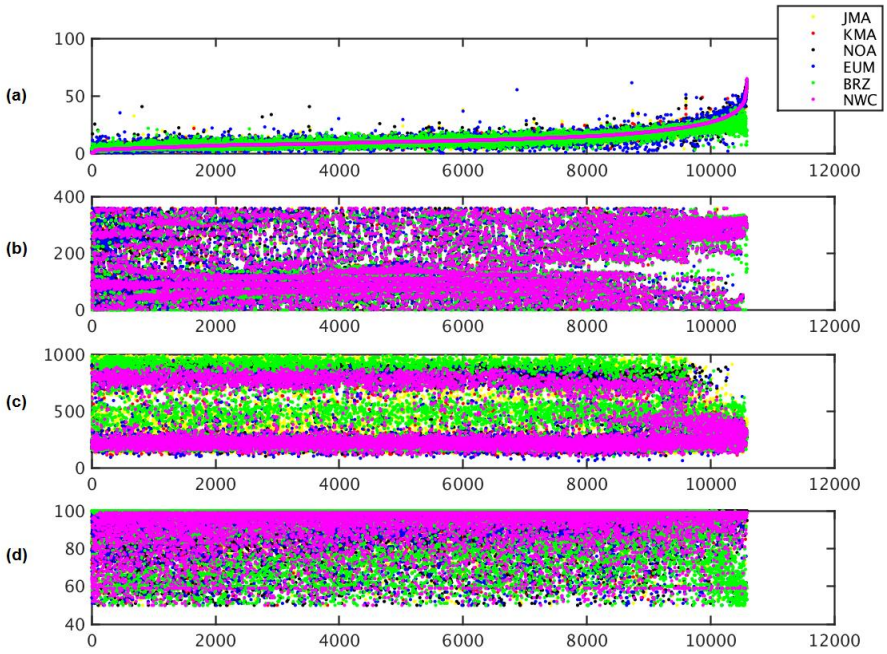

Figure 3. Parameter plot for Experiment 1 for collocated AMVs from the different AMV datasets, considering Common Quality Indicator >= 50% and a collocation distance up to 55 km. Considered variables are Speed (a), Direction (b), Pressure (c), and Common Quality Indicator (d). Colour codes correspond to BRZ in green, EUM in blue, JMA in yellow, KMA in red, NOA in black, NWC in magenta.

Collocated AMVs in **Figure 3** have been sorted by increasing speed for NWC. Some specific elements are here significant:

- EUM has many high-speed outliers (blue dots in **Figure 3a**). BRZ also has a cluster of low-speed outliers (green dots in the far right of the plot).
- Comparing with the previous "AMV Intercomparison" [15], the direction (**Figure 3b**) shows more easterlies even at high speeds, which is likely due to higher speed jets in the southern hemisphere during mid-winter (July), compared to September for that study.
- The pressure (**Figure 3c**) shows in general very few low-level AMVs with speeds greater than 20 m s^{-1}. Comparing with the previous "AMV Intercomparison" [15], there is a larger number of high-level AMVs with slow speeds at high levels, for which we cannot offer an explanation.
- Comparing the "Common Quality Indicator (CQI)" (**Figure 3d**) with that for the "Quality Indicator without forecast (QINF)" (not shown), there is more homogeneity between centers. This provides some evidence that the CQI gives better agreement in the AMVs, with a tendency to retain higher CQI values. On the other side, the generally lower CQI values for BRZ (green dots) may be related to the larger differences in the AMV pressure with the other centers.

Preprints (www.preprints.org) | NOT PEER-REVIEWED | Posted: 2 August 2019 doi:10.20944/preprints201908.0017.v1

Peer-reviewed version available at Remote Sens. 2019, 11, 2240; doi:10.3390/rs11192240

Considering in **Figure 4** the scatterplot of AMV pressures for collocated AMVs from the different centers versus EUM AMV pressures, with Common Quality Indicator (CQI) >= 50% and a collocation distance up to 55 km:

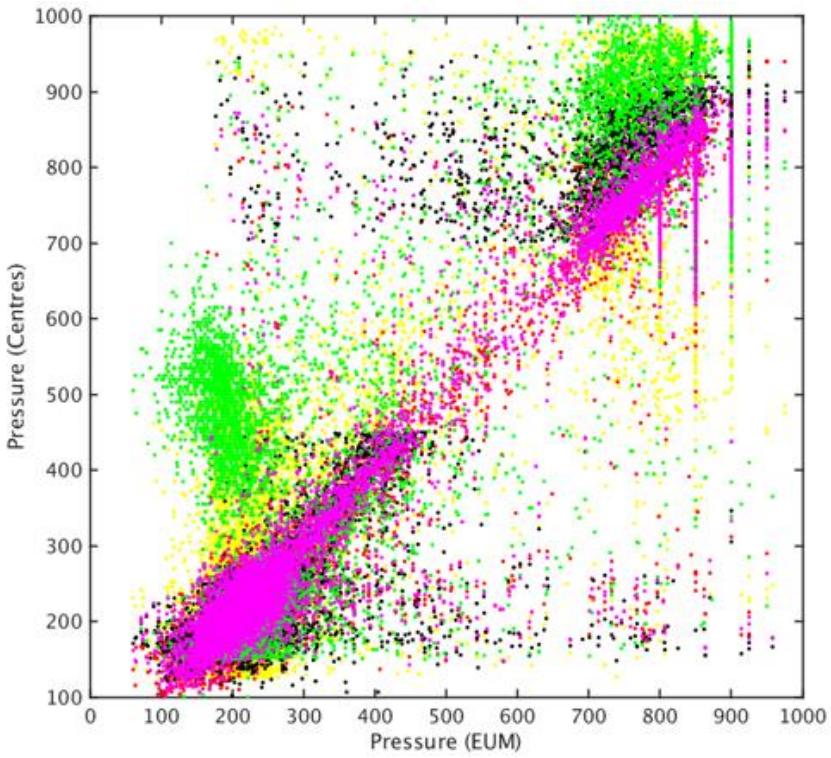

Figure 4. Scatterplot of collocated AMV pressures for Experiment 1, considering Common Quality Indicator >= 50% and a collocation distance up to 55 km, for each center versus EUM AMV pressures (BRZ in green; JMA in yellow; KMA in red; NOA in black; NWC in magenta).

The divergence in the AMV pressure values for the different centers is shown again, related to the different AMV height assignment methods. Three of these methods are based on the Cloud products (NOA, EUM, NWC; the two last ones using "CCC method" and so having the most similarities). The remainder use methods not based on the provided cloud product.

Considering this, in **Figure 4** there is excellent agreement between EUM and NWC (magenta clusters), many points plotted away from the diagonal (from the other centers), and large clusters of green dots (BRZ) away from the diagonal.

The updated AMV height assignment methods with respect to those in the previous "AMV Intercomparison" [15], define more variability in the AMV pressure values than the one shown then.

When the AMVs are compared to radiosonde winds (in **Table 3** using the threshold of 50%, and in **Table 4** using the threshold of 80% for the Common Quality Indicator), the best results are for JMA (with a vector RMS of 5 m s^{-1}), and then for NWC and NOA (with a vector RMS of 6-8 m s^{-1}). BRZ and EUM show poor results for the low-quality threshold, while much better for the high quality threshold, for which there is more homogeneity between centers.

In addition, there are important differences in the number of AMVs for the different centers despite using all of them the prescribed configuration.

Preprints (www.preprints.org) | NOT PEER-REVIEWED | Posted: 2 August 2019 doi:10.20944/preprints201908.0017.v1

Peer-reviewed version available at Remote Sens. 2019, 11, 2240; doi:10.3390/rs11192240

Table 3. Experiment 1: Comparison of AMVs with Common Quality Indicator >= 50%, to radiosonde winds within 150 km. (N = number of matches; Pre Bias = Pressure bias; Pre RMS = Pressure Root Mean Square Error; Spd Bias = wind speed bias; Spd RMS = wind speed Root Mean Square Error; Dir Bias = wind direction bias; Vec RMS = wind vector Root Mean Square Error). The extremes for each category are highlighted; in yellow the worst value and in green the best value.

	N	Pre Bias	Pre RMS	Spd Bias	Spd RMS	Dir Bias	Vec RMS
BRZ	774	0.90	14.68	-1.28	10.00	-13.13	12.61
EUM	443	-1.63	16.52	-1.74	7.86	8.69	12.67
JMA	400	0.50	13.81	-0.91	3.95	1.30	5.74
KMA	859	-0.55	15.16	-1.88	7.61	5.46	10.10
NOA	512	-1.05	14.15	-0.86	6.29	1.10	8.16
NWC	163	-0.69	15.11	-1.14	4.99	-1.47	6.80

Table 4. The same as **Table 3**, but with Common Quality Indicator >= 80%.

	N	Pre Bias	Pre RMS	Spd Bias	Spd RMS	Dir Bias	Vec RMS
BRZ	448	0.02	13.97	0.31	6.07	-14.61	8.62
EUM	312	-0.83	16.54	-1.79	6.54	8.31	8.56
JMA	344	0.78	13.77	-1.07	4.07	1.09	5.93
KMA	666	-0.79	15.51	-1.56	6.42	2.78	8.97
NOA	427	-1.49	13.96	-0.89	5.42	0.45	7.52
NWC	132	-0.41	15.08	-0.97	5.01	-5.98	6.94

Considering the comparison of collocated AMVs against the ECMWF ERA-Interim NWP analysis winds, in **Table 5** using the threshold of 80% for the Quality Indicator without Forecast (QINF) and in **Table 6** using the threshold of 80% for the Common Quality Indicator (CQI), the differences between centers are smaller, and even smaller using the CQI for the filtering.

JMA has again the best results, and only BRZ statistics are significantly worse than the rest. Although not shown, the situation is similar considering all AMVs altogether and the high and medium layer. At the low layer, BRZ statistics are better, leaving it in an intermediate position and EUM in the last position.

Table 5. Experiment 1: Comparison of collocated AMVs with Quality Indicator without Forecast (QINF) >= 80%, with NWP analysis winds. (N = number of AMVs; NBF = number of AMVs with Best fit pressure value; VD = Vector difference for all AMVs; VDBF = Vector difference for AMVs with Best fit pressure value; RMS = Root Mean Square Error for all AMVs; RMSBF = Root Mean Square Error for AMVs with Best Fit pressure value). The extremes for each category are highlighted; in yellow the worst value and in green the best value.

	N	NBF	VD	VDBF	RMS	RMSBF
BRZ	4930	1191	5.90	5.27	8.47	8.16
EUM	4930	1625	3.96	3.19	4.93	4.28
JMA	4930	1793	2.48	2.24	2.96	2.77
KMA	4930	1732	3.69	2.85	4.61	3.79
NOA	4930	1757	3.45	2.76	4.30	3.73
NWC	4930	1763	3.95	3.09	4.70	3.95

Preprints (www.preprints.org) | NOT PEER-REVIEWED | Posted: 2 August 2019 doi:10.20944/preprints201908.0017.v1

Peer-reviewed version available at Remote Sens. 2019, 11, 2240; doi:10.3390/rs11192240

Table 6. Experiment 1: The same as **Table 5**, but with Common Quality Indicator >= 80%.

	N	NBF	VD	VDBF	RMS	RMSBF
BRZ	8076	2122	5.54	4.85	7.53	7.13
EUM	8076	2655	4.04	3.24	4.97	4.28
JMA	8076	2860	2.59	2.33	3.10	2.89
KMA	8076	2802	3.80	2.97	4.73	3.94
NOA	8076	2854	3.54	2.82	4.36	3.74
NWC	8076	2791	3.99	3.17	4.74	4.03

Considering in **Table 7** an additional comparison of collocated AMVs against the NWP analysis winds, in which a different Common Quality Indicator (CQI) threshold is defined for each center so that a similar number of AMVs is kept for all of them (at least the 10,000 best AMVs):

Table 7. Experiment 1: Comparison of all AMVs to NWP analysis winds, with a Common Quality Indicator threshold so that at least 10000 AMVs are kept. (CQI = Common Quality Indicator threshold used for each center; N = number of AMVs; NBF = number of AMVs with Best fit pressure value; VD = Vector difference for all AMVs; VDBF = Vector difference for AMVs with Best fit pressure value; RMS = Root Mean Square Error for all AMVs; RMSBF = Root Mean Square Error for AMVs with Best Fit pressure value). The extremes for each category are highlighted; in yellow the worst value and in green the best value.

	CQI	N	NBF	VD	VDBF	RMS	RMSBF
BRZ	100	18355	3946	4.71	4.14	6.62	6.21
EUM	98	11120	3712	4.80	3.83	6.90	6.19
JMA	99	11805	4353	2.52	2.27	3.19	3.02
KMA	99	19170	7166	4.74	3.63	6.57	5.65
NOA	99	14086	5342	3.78	2.89	5.07	4.27
NWC	90	10117	3669	4.25	3.28	5.21	4.31

The CQI threshold ranges from 98% to 100% for all the centers except for NWC, for which it is 90%, as the total number of AMVs for NWC is much smaller than for the other centers in this Experiment 1. Despite the different criteria considered for this **Table 7**, the distribution of errors is not very different to that in **Tables 5 and 6**: JMA has again the best statistics, with NOA and NWC in later positions. The largest deviations are now being split between BRZ and EUM.

The distribution of the AMV pressure level against the AMV best fit pressure level is considered in **Figure 5**. The best fit pressure level has been computed for each AMV according to the method described by Salonen et al. (2012) [19].

This method defines the pressure for which the background NWP model wind has a minimum vector difference with the AMV wind. It does this by first determining the NWP model pressure level with a minimum vector difference between the AMV wind and the NWP wind.

Then, the actual minimum is calculated by using a parabolic fit to the vector difference for this model level and the levels directly above and below, which must be both less than or equal to 4 m s^{-1}, and at least 2 m s^{-1} smaller than the vector differences more than 100 hPa away from the best fit pressure level. Therefore, this method is dependent on the model vertical resolution.

Similar to previous studies, the number of best fit pressure level matches is for about 30% of the AMVs: depending on the AMV dataset, 21% to 36% of the AMVs are adjusted to a best fit pressure.

Peer-reviewed version available at Remote Sens. 2019, 11, 2240; doi:10.3390/rs11192240

Results show an approximate Gaussian distribution of the variable "AMV best fit pressure level - AMV pressure level" for all centers, which is more consistent than the one found in the previous "AMV Intercomparison" [15]. The pressure difference is centered near zero (upper panels in **Figure 5**) and extending up to ±200 hPa. The exception to this is JMA, for which the deviation is up to ±100 hPa only. This way, it is clear that JMA AMVs are much nearer to the AMV best fit pressure level than all other datasets. Although this may also indicate that the JMA AMV height assignment method has a stronger dependency on the NWP model background.

The maps in the lower panels of **Figure 5** depict the best fit displacements above (red) and below (blue) the AMV level for each AMV, which tend to be in similar locations for all centers for collocated AMVs. In the northern hemisphere, generally only high-level AMVs are adjusted, while in the southern hemisphere both high- and low-level clouds are adjusted to the best fit level.

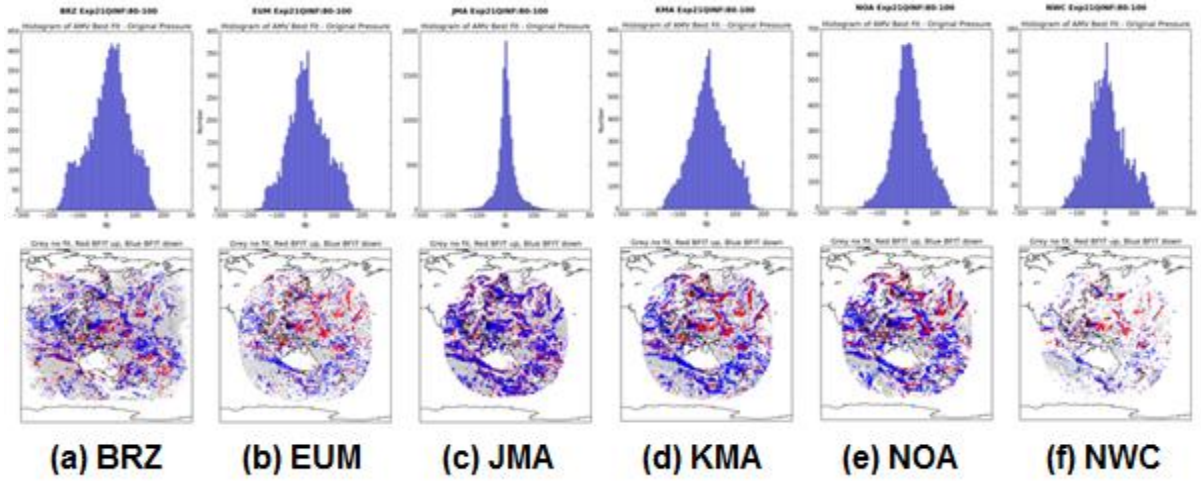

Figure 5. Experiment 1: Histogram and maps of "AMV best fit pressure level – AMV pressure level" for (a) BRZ, (b) EUM, (c) JMA, (d) KMA, (e) NOA, (f) NWC. In the maps, red shows the best fit pressure level is at a higher level; blue shows the best fit level is at a lower level.

Considering this, an additional calculation is defined to evaluate the difference between the AMV wind (before and after the best fit pressure level correction) and the NWP model wind. Results are shown in **Tables 8 and 9** for all AMVs for which the best fit pressure level correction could be applied, considering respectively a threshold of 80% for the Quality Indicator with forecast (QINF) and the Common Quality Indicator (CQI).

The speed bias is reduced in the case of BRZ, due to the significant value of this parameter before the best fit pressure level correction. For the rest of the centers, the speed bias was already small before the correction and so the impact of this correction in this parameter is not significant.

Considering the speed standard deviation, it is reduced about 70%-75% after the correction for all centers except for JMA, for which the reduction is only around 38%, as the JMA standard deviation before the best fit level correction is nearly as good as for the other centers after the best fit level correction.

Table 8. Experiment 1: Speed bias (BIAS) and Speed standard deviation (STD) with respect to the NWP analysis winds, before and after the best fit pressure level correction, for all AMVs with Quality Indicator without Forecast (QINF) >= 80% for which the best fit pressure level correction could be applied. The extremes for each category are highlighted; in yellow the worst value and in green the best value.

	BIAS before	STD before	BIAS after	STD after
BRZ	-1.00	4.38	0.28	1.16
EUM	-0.15	4.65	0.26	1.19
JMA	0.06	1.79	0.21	1.11
KMA	-0.12	4.42	0.21	1.14
NOA	-0.04	3.77	0.23	1.17
NWC	0.13	3.97	0.27	1.18

Table 9. The same as **Table 8**, but with Common Quality Indicator (CQI) >= 80%.

	BIAS before	STD before	BIAS after	STD after
BRZ	-1.12	4.33	0.25	1.16
EUM	-0.20	4.57	0.26	1.18
JMA	0.05	1.78	0.22	1.11
KMA	-0.33	4.55	0.21	1.14
NOA	-0.04	3.77	0.23	1.17
NWC	-0.25	4.01	0.23	1.16

Preprints (www.preprints.org) | NOT PEER-REVIEWED | Posted: 2 August 2019 doi:10.20944/preprints201908.0017.v1

Peer-reviewed version available at Remote Sens. 2019, 11, 2240; doi:10.3390/rs11192240

3.2. Experiment 2

In this case, AMV producers extracted cloudy AMVs with the Himawari-8/AHI IR10.4 μm triplet 1200-1220 UTC, using their best options for the AMV calculation, and considering their specific configuration for target box sizes, search scene sizes and target locations. This way, differences of each AMV extraction process with respect to the previous prescribed configuration can be compared.

Considering in **Table 10** the parameter distribution for the AMV datasets, with Common Quality Indicator (CQI) >= 50%:

Table 10. Parameter distribution for Experiment 2 for the different AMV datasets, considering Common Quality Indicator (CQI) >= 50%:

	BRZ	EUM	JMA	KMA	NOA	NWC
Total AMVs	74100	30806	67324	53171	47320	146780
CQI >= 50%	65673	28174	27057	47411	45782	146496
SPD_min (m/s)	2.55	2.50	2.51	2.50	3.00	2.50
SPD_max (m/s)	70.06	145.55	85.94	97.01	94.16	84.03
SPD_mean (m/s)	12.02	13.37	14.00	13.89	13.97	12.97
P_min (hPa)	100.00	57.58	125.02	106.81	105.72	101.00
P_max (hPa)	1000.00	1009.80	996.47	1000.00	987.20	972.50
P_mean (hPa)	487.06	438.03	497.74	450.50	432.01	409.12
Low_AMVs (%)	29.96	27.15	32.27	24.56	33.55	25.63
Mid_AMVs (%)	21.19	14.14	17.51	22.02	2.56	11.52
High_AMVs (%)	48.85	58.71	50.22	53.42	63.89	62.86
Low_SPD_min (m/s)	2.55	2.50	2.51	2.50	3.01	2.50
Low_SPD_max (m/s)	46.46	54.21	32.67	70.27	37.59	36.22
Low_SPD_mean (m/s)	9.39	8.89	9.14	10.54	9.77	8.76
Low_P_min (hPa)	700.00	700.06	700.04	700.00	700.08	700.00
Low_P_max (hPa)	1000.00	1009.80	996.47	1000.00	987.20	972.50
Low_P_mean (hPa)	870.56	820.69	887.37	817.99	835.02	788.38
Mid_SPD_min (m/s)	2.55	2.51	2.51	2.50	3.04	2.51
Mid_SPD_max (m/s)	69.46	69.67	72.05	80.01	69.25	62.00
Mid_SPD_mean (m/s)	13.73	13.95	14.46	15.11	21.30	14.95
Mid_P_min (hPa)	400.03	400.06	400.00	400.02	400.06	400.50
Mid_P_max (hPa)	699.97	699.73	699.97	699.98	449.98	699.50
Mid_P_mean (hPa)	528.14	529.96	533.05	514.73	426.70	535.47
High_SPD_min (m/s)	2.59	2.50	2.52	2.50	3.00	2.50
High_SPD_max (m/s)	70.06	145.55	85.94	97.01	94.16	84.03
High_SPD_mean (m/s)	12.88	15.31	16.97	14.92	15.88	14.33
High_P_min (hPa)	100.00	57.58	125.02	106.81	105.72	101.00
High_P_max (hPa)	400.00	399.94	399.98	400.00	399.97	400.00
High_P_mean (hPa)	233.99	238.96	235.09	255.08	220.57	231.35

- The total number of AMVs ranges from 47,000 to 74,000, with lower values for EUM (31,000), and higher values for NWC (147,000). Comparing with Experiment 1, the difference in the total number of AMVs is small for all centers (only up to 25%) except for NWC, for which the total number of AMVs is one order of magnitude larger. The differences with Experiment 1 are caused by the specific configuration of each center for the target box sizes, search scene sizes and target locations.

Peer-reviewed version available at Remote Sens. 2019, 11, 2240; doi:10.3390/rs11192240

- The number of AMVs is much larger with Himawari satellites than in the previous "AMV Intercomparison" with MSG satellite [15], which found up to approximately 10,000 AMVs (although KMA was then able to calculate 50,000 AMVs and NWC was able to calculate 90,000 AMVs). As already said, this is due, in part, to the higher resolution of Himawari/AHI (2 km) versus MSG/SEVIRI (3 km), more oceanic regions, and fewer deserts.
- The maximum speed ranges from 80 m s^{-1} (BRZ) to 97 m s^{-1} (KMA), with outliers of 146 m s^{-1} again for EUM.
- The minimum pressure is around 100 hPa, except for EUM which is again at 58 hPa.
- The percentage of AMVs by layer (low layer between 700 and 1000 hPa, medium layer between 400 and 700 hPa, and high layer between 100 and 400 hPa) are respectively 25% to 34%, 12% to 22%, and 49% to 64%. The main outlier of these is NOA again at medium levels with only 3%.

Figure 6 shows the spatial localization of AMVs inside the Himawari-8 Full Disk, and the distribution of parameters (Common Quality Indicator, Speed, Direction and Pressure) for the different AMV datasets, considering Common Quality Indicator (CQI) >= 50%:

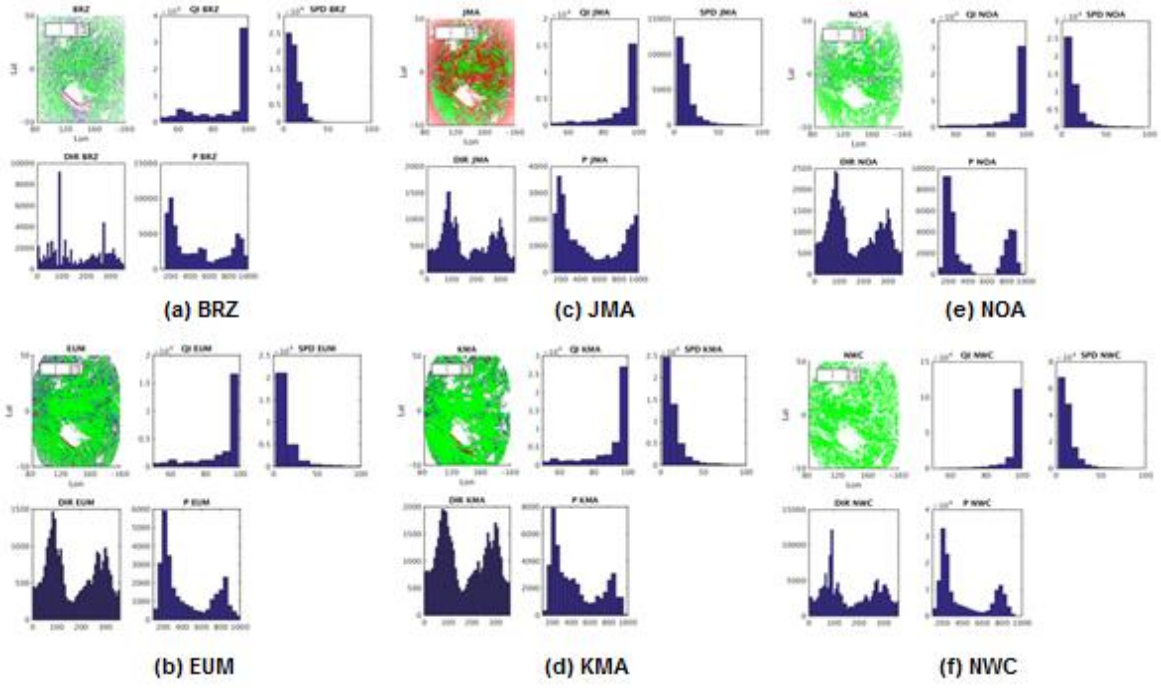

Figure 6. AMV spatial localization and Distribution of parameters for Experiment 2 considering Common Quality Indicator (CQI) >= 50% (Common Quality Indicator, Speed, Direction, Pressure) for the different AMV datasets: (a) BRZ, (b) EUM, (c) JMA, (d) KMA, (e) NOA, (f) NWC.

The parameter distributions are very similar to those for Experiment 1 in **Figure 2**, and so the same conclusions are to be taken into account. Specifically, the distribution of the Common Quality Indicator (CQI) values looks similar for all centers again. The differences in the height assignment process drive again the majority of differences observed in the AMV datasets.

Preprints (www.preprints.org) | NOT PEER-REVIEWED | Posted: 2 August 2019 doi:10.20944/preprints201908.0017.v1

Peer-reviewed version available at Remote Sens. 2019, 11, 2240; doi:10.3390/rs11192240

Considering in **Figure** 7 the parameter plot for different variables for collocated AMVs from the different centers with Common Quality Indicator (CQI) >= 50% and a collocation distance up to 55 km:

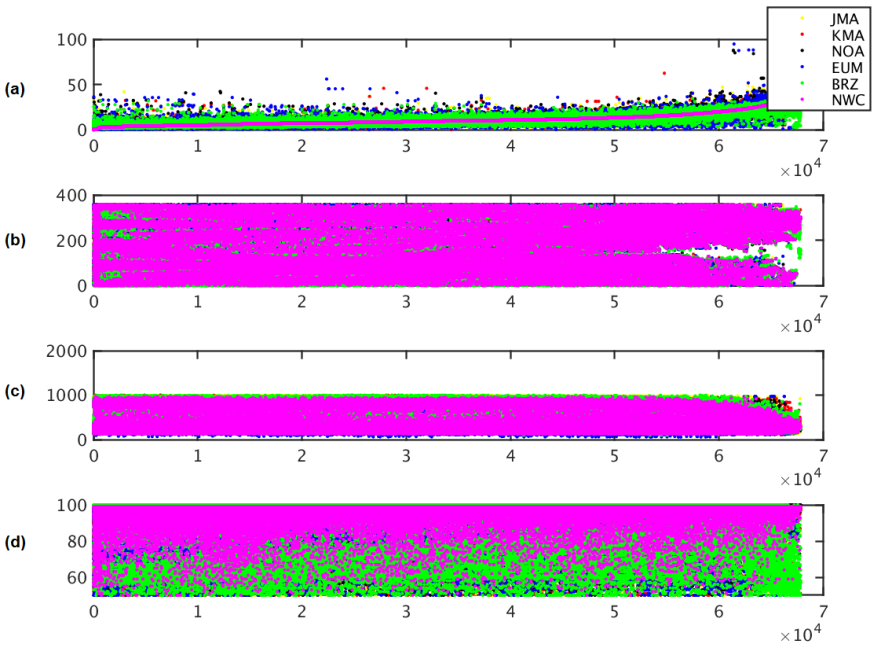

Figure 7. Parameter plot for Experiment 2 for collocated AMVs from the different AMV datasets, considering Common Quality Indicator (CQI) >= 50% and a collocation distance up to 55 km. Considered variables are Speed (a), Direction (b), Pressure (c), and Common Quality Indicator (d). Colour codes correspond to BRZ in green, EUM in blue, JMA in yellow, KMA in red, NOA in black, NWC in magenta.

Collocated AMVs in **Figure 7** have been sorted by increasing speed for NWC. In general, **Figure 7** is in agreement with **Figure 3** for Experiment 1 of this study:

- Considering the speed plot in **Figure 7a**, the EUM high-speed outliers (blue dots), and the BRZ cluster of low-speed outliers (green dots in the far right of the plot) detected in Experiment 1 are seen again.
- Considering the Common Quality Indicator (CQI) plot in **Figure 7d**, there is again a tendency to retain high CQI values for all centers except BRZ, for which its lower CQI values (green dots in the plot) may be related to the larger differences in AMV pressure with the other centers.
- The other graphs in **Figure 7** are however dominated by the nearly 150,000 AMVs from NWC, because of which additional information cannot be extracted.

Preprints (www.preprints.org) | NOT PEER-REVIEWED | Posted: 2 August 2019 doi:10.20944/preprints201908.0017.v1

Peer-reviewed version available at Remote Sens. 2019, 11, 2240; doi:10.3390/rs11192240

Considering in **Figure 8** the scatterplot of AMV pressures for collocated AMVs from the different centers versus EUM AMV pressures, with Common Quality Indicator (CQI) >= 50% and a collocation distance up to 55 km:

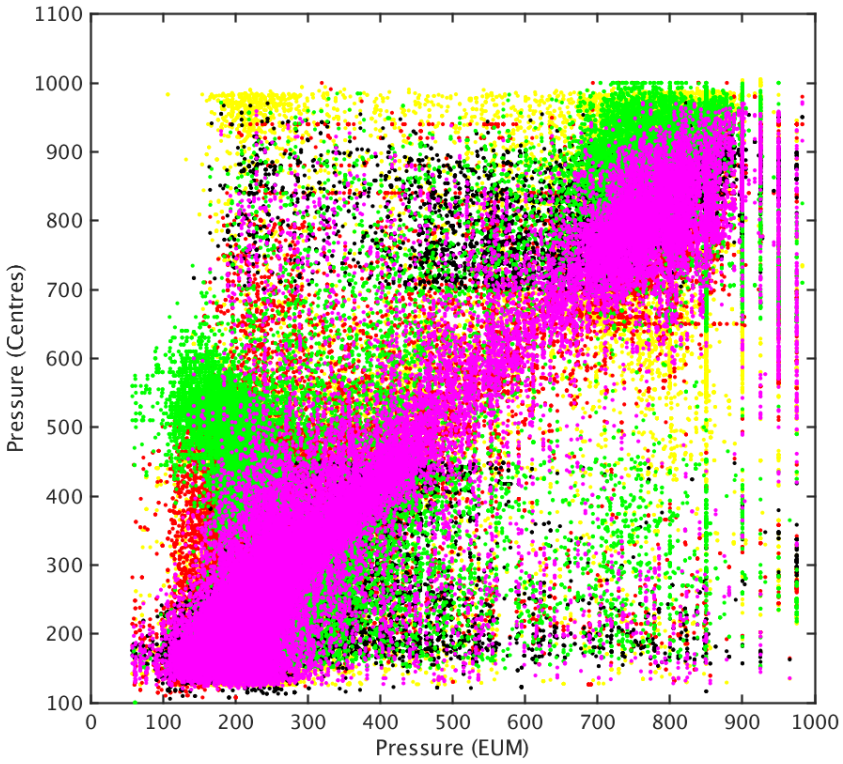

Figure 8. Scatterplot of collocated AMV pressures for Experiment 2, considering Common Quality Indicator (CQI) >= 50% and a collocation distance up to 55 km, for each center versus EUM AMV pressures (BRZ in green; JMA in yellow; KMA in red; NOA in black; NWC in magenta).

Figure 8 is in agreement with **Figure 4** for Experiment 1 of this study, but with a much larger number of AMV collocations between centers.

There is again an excellent agreement between EUM and NWC (magenta clusters), and many points plotted away from the diagonal (from the other centers). There are large clusters of green dots related to BRZ away from the diagonal, based on the different height assignment method used. This partially also occurs with some black dots related to NOA, with a higher concentration of its AMVs in the highest layer (< 250 hPa) and the lowest layer (>700 hPa).

When the AMVs are compared to radiosonde winds (in **Table 11** using the threshold of 50%, and in **Table 12** using the threshold of 80% for the Common Quality Indicator (CQI)), the best results are again for JMA (with a vector RMS of 6 m s^{-1}), and then for NOA and NWC (with a vector RMS of 7 m s^{-1}). EUM results are much better in Experiment 2, using their specific configuration. The higher quality threshold in **Table 12** contributes again to more homogeneity in the statistics of the different centers.

Preprints (www.preprints.org) | NOT PEER-REVIEWED | Posted: 2 August 2019 doi:10.20944/preprints201908.0017.v1

Peer-reviewed version available at Remote Sens. 2019, 11, 2240; doi:10.3390/rs11192240

Table 11. Experiment 2: Comparison of AMVs with Common Quality indicator (CQI) >= 50%, to radiosonde winds within 150 km. (N = number of matches; Pre Bias = Pressure bias; Pre RMS = Pressure Root Mean Square Error; Spd Bias = wind speed bias; Spd RMS = wind speed Root Mean Square Error; Dir Bias = wind direction bias; Vec RMS = wind vector Root Mean Square Error). The extremes for each category are highlighted; in yellow the worst value and in green the best value.

	N	Pre Bias	Pre RMS	Spd Bias	Spd RMS	Dir Bias	Vec RMS
BRZ	942	1.46	14.44	-2.69	11.65	-9.48	15.22
EUM	508	-0.62	15.92	-2.17	7.03	10.08	8.87
JMA	313	-2.94	18.33	-1.36	4.64	-0.83	6.34
KMA	797	-0.64	14.80	-1.55	7.78	-1.41	10.03
NOA	691	-1.58	13.93	-0.90	5.44	1.89	7.62
NWC	2204	-1.02	16.30	-2.17	6.03	0.40	7.85

Table 12. The same as **Table 11**, but with Common Quality indicator (CQI) >= 80%.

	N	Pre Bias	Pre RMS	Spd Bias	Spd RMS	Dir Bias	Vec RMS
BRZ	619	1.16	13.44	-0.40	7.36	-14.65	9.80
EUM	366	-0.66	14.74	-2.20	6.15	8.43	8.56
JMA	270	-3.43	18.67	-1.40	4.64	-0.83	5.93
KMA	628	-0.84	14.30	-1.21	7.39	-2.66	8.97
NOA	599	-1.69	13.98	-0.88	5.25	0.39	7.52
NWC	2063	-1.19	16.19	-2.11	5.99	0.79	6.94

Considering the comparison of collocated AMVs against the ECMWF ERA-Interim NWP analysis winds, in **Table 13** with for the Quality Indicator with forecast (QINF) >= 80%, and in **Table 14** with Common Quality Indicator (CQI) >= 80%, differences between centers are smaller.

Table 13. Experiment 2: Comparison of collocated AMVs with Quality Indicator without Forecast (QINF) >= 80%, to NWP analysis winds. (N = number of AMVs; NBF = number of AMVs with Best fit pressure value; VD = Vector difference for all AMVs; VDBF = Vector difference for AMVs with Best fit pressure value; RMS = Root Mean Square Error for all AMVs; RMSBF = Root Mean Square Error for AMVs with Best Fit pressure value. The extremes for each category are highlighted; in yellow the worst value and in green the best value.

	N	NBF	VD	VDBF	RMS	RMSBF
BRZ	43281	9814	5.60	5.01	8.20	7.90
EUM	43281	13270	3.84	3.05	4.96	4.24
JMA	43281	14572	2.20	1.99	2.71	2.52
KMA	43281	12709	3.75	3.08	5.05	4.51
NOA	43281	13765	3.41	2.74	4.26	3.64
NWC	43281	13588	3.45	2.79	4.13	3.54

Table 14. Experiment 2: The same as **Table 13**, but with CQI >= 80%.

	N	NBF	VD	VDBF	RMS	RMSBF
BRZ	56515	13075	5.73	5.11	8.35	8.02
EUM	56515	17533	4.00	3.17	5.17	4.43
JMA	56515	19208	2.27	2.06	2.80	2.62
KMA	56515	16635	3.92	3.23	5.25	4.72
NOA	56515	18163	3.53	2.84	4.42	3.80
NWC	56515	17860	3.55	2.87	4.24	3.65

In **Tables 13 and 14**, JMA has again the best results and only BRZ statistics are again significantly worse. Although not shown, the situation is similar considering all AMVs altogether and the high and medium layer. At the low layer, BRZ statistics are better, leaving it in an intermediate position and leaving KMA in the last position.

Considering in **Table 15** the additional comparison of collocated AMVs against the NWP analysis winds, in which a different Common Quality Indicator (CQI) threshold is defined for each center, so that a similar number of AMVs is kept for all of them (at least the 10,000 best AMVs):

Table 15. Experiment 2: Comparison of all AMVs to NWP analysis winds, with a Common Quality Indicator (CQI) threshold, so that at least 10000 AMVs are kept. (CQI = Common Quality Indicator threshold used for each center; N = number of AMVs; NBF = number of AMVs with Best fit pressure value; VD = Vector difference for all AMVs; VDBF = Vector difference for AMVs with Best fit pressure value; RMS = Root Mean Square Error for all AMVs; RMSBF = Root Mean Square Error for AMVs with Best Fit pressure value). The extremes for each category are highlighted; in yellow the worst value and in green the best value.

	CQI	N	NBF	VD	VDBF	RMS	RMSBF
BRZ	100	26341	5733	5.90	5.22	8.32	7.91
EUM	98	12407	4056	4.43	3.46	6.13	5.28
JMA	98	10595	3991	2.52	2.29	3.20	3.03
KMA	99	16721	5934	4.66	3.75	6.71	6.06
NOA	100	14484	5484	3.84	2.91	5.06	4.21
NWC	99	80625	28532	4.24	3.26	5.24	4.36

The Common Quality Indicator (CQI) threshold ranges from 98% to 100% for all the centers. Despite the different criteria considered for this **Table 15**, the distribution of errors is similar to those in **Tables 13 and 14**: JMA has again the best statistics, with NOA and NWC in later positions. The largest deviations are related again to BRZ.

The distribution of the AMV pressure level against the AMV best fit pressure level, computed again as described for Experiment 1 in **Figure 5**, is considered now for Experiment 2 in **Figure 9**.

Similarly, the number of best fit pressure level matches is for 22% to 38% of the AMVs, depending on the AMV dataset. Results show again the approximate Gaussian distribution of the variable "AMV best fit pressure level - AMV pressure level" for all centers.

The pressure difference is centered again near zero (upper panels in **Figure 9**), extending up to ±200 hPa, except for JMA for which the deviation is up to ±100 hPa only.

This way, it is again clearer that JMA AMVs are much closer to the AMV best fit level than all other datasets. Although with a possibly stronger dependency on the NWP model background.

The maps in the lower panels of **Figure 9** depict anew the best fit displacements above (red) and below (blue) the AMV level for each AMV. Again, they tend to be in similar locations for all centers for collocated AMVs.

Preprints (www.preprints.org) | NOT PEER-REVIEWED | Posted: 2 August 2019 doi:10.20944/preprints201908.0017.v1

Peer-reviewed version available at Remote Sens. 2019, 11, 2240; doi:10.3390/rs11192240

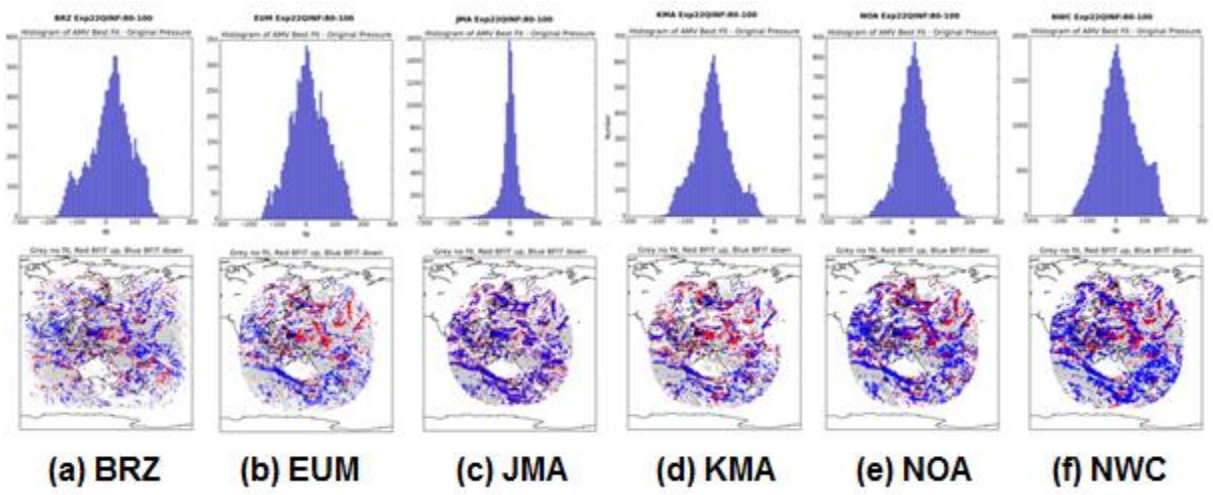

Figure 9. Experiment 2: Histogram and maps of "AMV best fit pressure – original AMV pressure" for (a) BRZ, (b) EUM, (c) JMA, (d) KMA, (e) NOA, (f) NWC. In the maps, red shows the best fit pressure level is at a higher level; blue shows the best fit level is at a lower level.

Considering this, the additional calculation to evaluate the difference between the AMV wind (before and after the best fit pressure level correction) and the NWP model wind, is defined again. Results are shown in **Tables 16 and 17** for all AMVs for which the best fit pressure level correction could be applied, considering respectively Quality Indicator with forecast (QINF) >= 80% and Common Quality Indicator (CQI) >= 80%.

Table 16. Experiment 2: Speed bias (BIAS) and Speed standard deviation (STD) with respect to the NWP analysis winds, before and after the best fit pressure level correction, for all AMVs with Quality Indicator without Forecast (QINF) >= 80%, for which the best fit pressure level correction could be applied. The extremes for each category are highlighted; in yellow the worst value and in green the best value.

	BIAS before	STD before	BIAS after	STD after
BRZ	-1.51	4.57	0.26	1.17
EUM	-0.28	4.60	0.18	1.17
JMA	0.09	1.82	0.20	1.14
KMA	0.65	3.89	0.23	1.14
NOA	-0.22	3.82	0.24	1.15
NWC	-0.32	3.94	0.20	1.14

Table 17. The same as **Table 16**, but with Common Quality Indicator (CQI) >= 80%.

	BIAS before	STD before	BIAS after	STD after
BRZ	-1.57	4.56	0.26	1.16
EUM	-0.20	4.57	0.26	1.18
JMA	0.07	1.82	0.21	1.12
KMA	0.60	3.97	0.22	1.15
NOA	-0.22	3.82	0.24	1.15
NWC	-0.68	4.10	0.18	1.12

556 The speed bias is reduced in the cases of BRZ, KMA and NWC. For the rest of the centers, the
557 speed bias was already small before the correction and so the impact of this correction in this
558 parameter is not significant.
559 Considering the speed standard deviation, again it is reduced around 70%-75% after the
560 correction for all centers except for JMA, for which the reduction is around 38%, as the JMA standard
561 deviation before the best fit level correction was nearly as good as for the other centers after the best
562 fit level correction.
563
564

3.3 Experiment 3

In this case producers extracted AMVs with the Himawari-8/AHI IR10.4 μm triplet for 21 July 2016 0530-0550 UTC, considering their best options for AMV calculation and their specific configurations for target box size, search scene size and target location (as in Experiment 2). This dataset is used for validation against NASA's CALIPSO (Cloud-Aerosol Lidar and Infrared Pathfinder Satellite Observation), which provides an independent measurement of cloud top height.

CALIPSO is a line-of-site measurement, so there are few collocations with AMVs (tens of matches only). Therefore, this evaluation is qualitative as illustrated in the following **Figures 10 and 11**. The thresholds for determining collocation are a distance of 0.1 degree for latitude and longitude, and a time of one hour.

All previous analysis of variables, validation against radiosonde wind data and NWP analysis wind data, and best fit analysis done for Experiment 2 are not repeated again here, as both experiments are as said equivalent.

Figure 10 contains the following plots and information for the CALIPSO data for 21 July 2016 0530-0550 UTC, used in Experiment 3:

- The first panel shows the CALIPSO ground track (red line) for the case, over a map of the West Pacific Ocean.
- The second panel is the same ground track superimposed over an RGB image of the corresponding Himawari-8 image.
- The third panel is similar to the second one, excepting that the underlying image is the Himawari-8 derived cloud top height product.
- The last panel contains some statistics for the CALIPSO data.

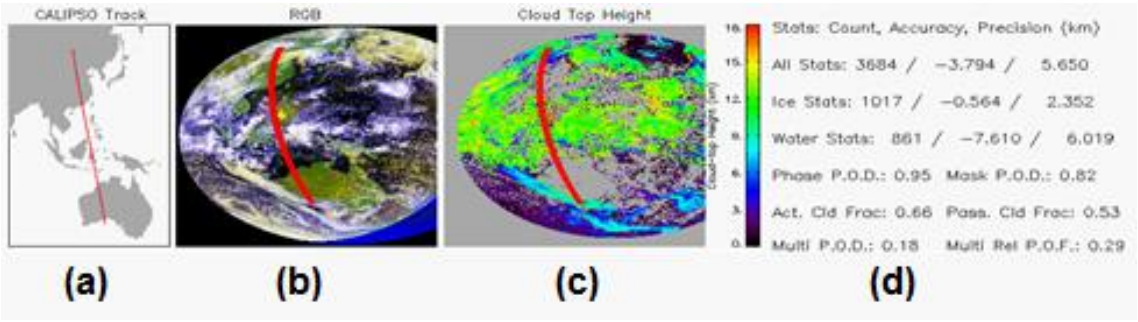

Figure 10. CALIPSO data for 21 July 2016 at 0530-0550 UTC, used in Experiment 3: (a) Ground track over a map of the West Pacific Ocean, (b) Ground track over the corresponding Himawari-8 RGB image, (c) Ground track over the corresponding Himawari-8 derived Cloud top height, (d) Statistics for the CALIPSO data.

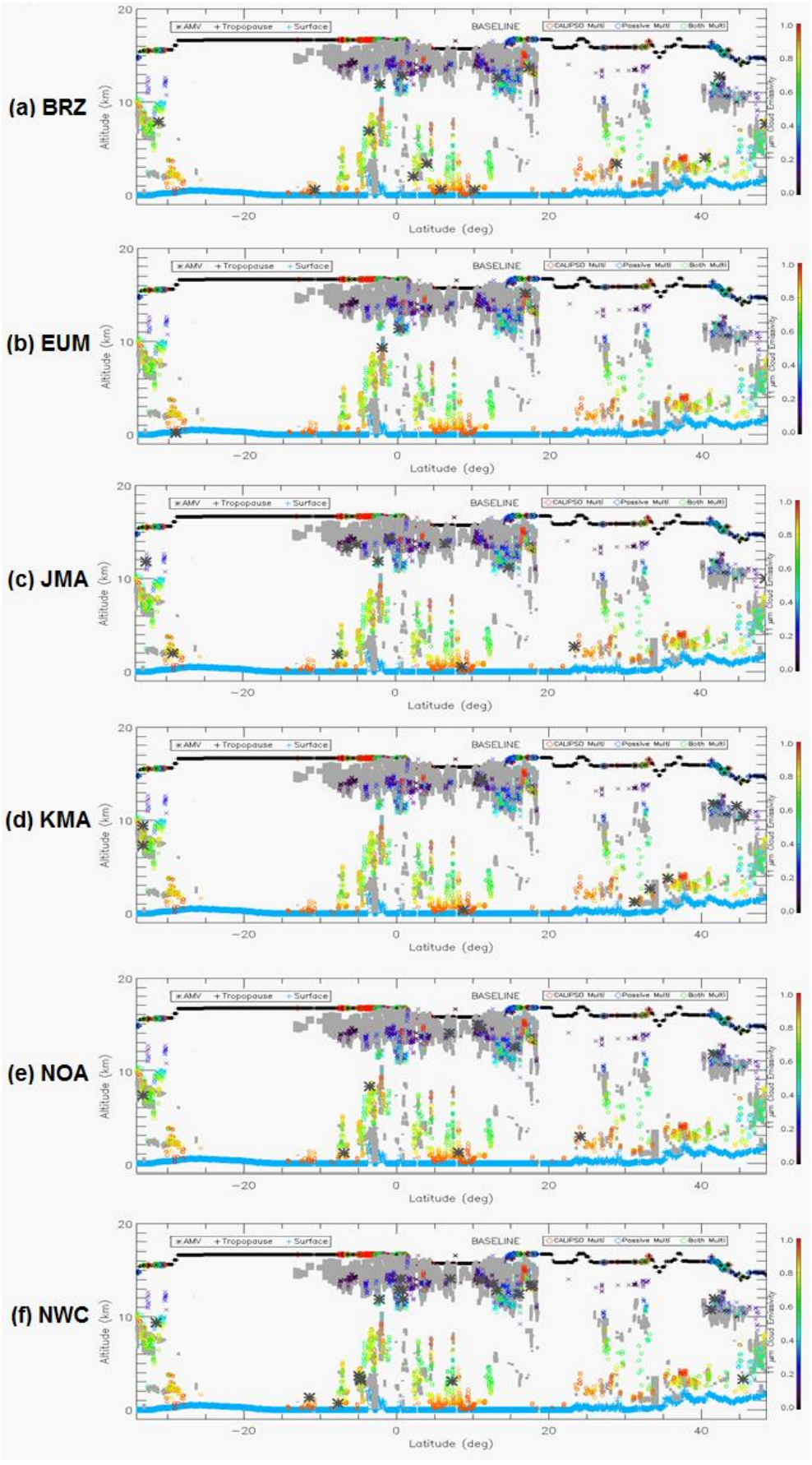

Figure 11. Experiment 3: Collocation of AMVs (defined as black asterisks *), with CALIPSO cloud measurements for (a) BRZ, (B) EUM, (c) JMA, (d) KMA, (e) NOA, (f) NWC.

596 **Figure 11** depicts for the different centers the clouds as detected by CALIPSO (colour-coded
597 from gray to red by emissivity). The tropopause height is designated by the black line across the top
598 of the graph (near the top of the cirrus clouds). The topography of the Earth's surface is the light blue
599 line in the lower part of the graph. In each one of the panels, the collocated AMVs for each center are
600 shown as black asterisk symbols, primarily located near the base of the cirrus cloud feature in the
601 middle of the graph, and at the top the low level and medium level clouds located in the central and
602 right side of the graph.
603
604 Overall, the results are in general agreement with the best fit analysis in Experiment 2, as in
605 general the high level AMVs need to be adjusted higher in the atmosphere.
606 AMV heights for the different centers are in good agreement in this specific example, in
607 apparent disagreement with the previous AMV pressure scatter plots. However, this is a very small
608 sample and no attempt was made to ensure that the AMVs are collocated: data from each center
609 were plotted independently from the others.
610

3.4 Similarities in the AMV datasets

To quantify the differences observed in the AMV datasets in Experiments 1 and 2, a "paired t-test" was used with all combinations of AMV datasets and four considered parameters (speed, direction, pressure and quality indicator), to determine if the differences in the parameters are statistically significant for collocated pairs of AMVs. This is done because there is no "ground truth" for AMVs, and one of the goals of this study is to determine the similarity in the AMVs from the different centers.

The statistics are computed using the "MATLAB paired t-test" function which performs a "t-test" of the hypothesis that the data come from a distribution with mean zero. The data used here were the differences in each parameter from each pair of AMV datasets; therefore, a mean of zero is expected.

AMVs used with this t-test are quality controlled, retaining only those with Quality Indicator without forecast (QINF) >= 50% and >= 80%, and also those with Common Quality Indicator (CQI) >= 50% and 80%. For collocation, the distance used here between AMVs is up to 35 km.

Tables 18 and 19 show respectively for Experiment 1 (with prescribed configuration) and for Experiment 2 (with specific configuration), the pairs of combinations with parameter differences not statistically significant. A total of 15 combinations is defined per parameter (considering all combinations of AMV datasets), and so a total of 60 combinations is defined in each whole test.

Table 18. Similarities found in the AMV datasets by the "paired t-test" for the different combinations of variables and AMV datasets, in Experiment 1 (with prescribed configuration).

Prescribed Configuration	Speed	Direction	Pressure	Quality Indicator	ALL
QINF >= 50%	4	6	1	0	11
QINF >= 80%	6	6	1	1	14
CQI >= 50%	2	1	0	1	4
CQI >= 80%	2	6	1	1	10

Table 19. Similarities found in the AMV datasets by the "paired t-test" for the different combinations of variables and AMV datasets, in Experiment 2 (with specific configuration).

Specific Configuration	Speed	Direction	Pressure	Quality Indicator	ALL
QINF >= 50%	1	2	0	0	3
QINF >= 80%	1	2	2	0	5
CQI >= 50%	1	2	0	0	3
CQI >= 80%	1	1	0	1	3

The most consistent agreement is for the AMV direction with the prescribed configuration and the high quality indicator thresholds. The similarities then reduce progressively for the AMV speed, and the AMV quality indicator and pressure. The lack of agreement in the AMV pressure is likely due to the lack of commonality in the AMV height assignment algorithms; here, though both EUM and NWC centers use CCC method for the height assignment, there are still significant differences for this variable even for these centers.

643 In general, more homogeneity between variables in different datasets is seen using the same
644 prescribed configuration, using a higher Quality indicator threshold in the AMV filterings, and
645 using the specific "Quality Indicator with forecast (QINF)" calculated by each center.
646 This last result seems to be in contradiction with elements shown in the previous sections, in
647 which the "Common Quality Indicator (CQI)" provided more homogeneity in the AMV statistics of
648 different centers (comparing for example **Tables 5 and 6**).
649 The result here can be however derived from the fact that, with the "Common Quality Indicator
650 (CQI)" the AMV samples of data for all centers are larger, and with this the "paired t-test" has more
651 difficulties to show a mean of zero in its distribution.
652

4. Conclusions

The following are general observations, conclusions, and recommendations from this "AMV Intercomparison Study":

1) Experiments 1 and 2 only differed in terms of a prescribed versus specific configuration. Overall, the results between the two experiments were nearly the same in terms of bulk statistics, collocated statistics, comparisons to radiosonde winds and NWP analysis winds and best fit analysis, with the main variations related to the number of calculated AMVs. This implies that the impact of using a prescribed versus a specific configuration is small.
2) For the experiments, the centers used the AMV height assignment method of their choice. This height assignment method has the biggest impact in the lack of agreement in the AMVs.
3) The Common Quality Indicator (CQI) was introduced in this Intercomparison, and it showed some skill in filtering collocated AMVs, resulting in an improved statistical agreement.
4) Another first for this study is the addition of CALIPSO data to provide an independent measurement of cloud height, to be used for comparison and validation of the AMV heights. Due to the small sample of collocated observations for the comparison, only a qualitative assessment could be made: AMV heights were generally near the cloud base for the high-level thin cirrus clouds, and near the cloud top for low and medium level clouds detected by CALIPSO. For the next round of AMV Intercomparison studies, a comparison of AMVs with MISR winds is planned for additional checkings of the AMVs and the AMV heights.
5) Even though there was a large variation in the AMV heights for collocated winds, the best fit analysis and CALIPSO comparison both show that there are equivalent, high quality winds produced by all centers. This may indicate that the quality control post-processing by each center is an important step in filtering out poor quality AMVs, so resulting in a higher quality product. For future intercomparison studies, an experiment to substantiate this conjecture should be considered.

The following sections detail the findings from the experiments, in terms of each AMV producer independently. This includes the strengths and weaknesses as determined from the results of the experiments:

(a) BRZ - Brazil Center for Weather Prediction and Climate Studies (CPTEC/INPE)

The performance of the BRZ AMV algorithm has improved with respect to the results in the previous AMV intercomparison. Results are more in agreement with the rest of AMV centers, and differences in many of the variables have reduced.

In any case, it is clear that there still exists room for improvement. On one hand, there are still large differences in the AMV height assignment, as compared to all other centers. This results in BRZ often having the largest deviations from radiosonde winds and NWP analysis winds. On the other hand, BRZ has still to verify the differences found in the direction histograms, in which some directions are found to be much more frequent than other ones.

(b) KMA - Korea Meteorological Administration

The KMA algorithm performed similarly to the results from the previous AMV intercomparison. Overall, the comparisons to radiosonde winds and NWP analysis winds were in the middle of the distributions.

(c) EUM - European Organization for the Exploitation of Meteorological Satellites (EUMETSAT)

The behavior of EUM algorithm was much better when the Quality Indicator threshold used was high (80%), and when its specific configuration was used (comparing with the results with the prescribed configuration). In these circumstances, the performance of EUM AMVs is basically similar to that of other centers (NOA or NWC).

The similarities in the height assignment of EUM and NWC centers are also to be noticed, due to the fact of both using the same "CCC method height assignment".

(d) NOA – United States National Oceanic and Atmospheric Administration (NOAA)

Results for the NOA algorithm have much improved with respect to the previous Intercomparison study, and now their validation results against radiosonde winds and NWP analysis winds are in second position (together with NWC). In any case, there are still some issues with the NOAA algorithm, for example the vertical distribution of the AMVs, for which there are very few AMVs in middle levels, which is in disagreement with the rest of the centers.

(e) NWC – Satellite Application Facility on support to Nowcasting (NWCSAF)

NWC algorithm agrees well with other centers in terms of parameter distributions, especially when using the Common Quality Indicator and its specific configuration. Its validation results against radiosonde winds and NWP analysis winds are in second position (together with NOA).

The NWC algorithm is basically the same as the one used for the previous AMV Intercomparison. Due to this stability, its overall performance is similar to what was found in that previous AMV Intercomparison study.

However, some elements have been detected that need some analysis by NWC AMV producers: the fact that some AMV directions (e.g., 90°) are more frequent in the direction histogram than others in their vicinity.

(f) JMA - Japan Meteorological Agency

JMA algorithm is the one with best performance, considering in general all validation and checking elements. This reflects the most important change in all AMV algorithms when compared to the previous AMV Intercomparison. Specifically, they have the best overall statistics when compared to radiosonde winds and NWP analysis winds, and their best fit analysis shows that the differences with respect to the best fit level for JMA AMVs are much smaller than for other centers.

All this is most likely due to the updated JMA AMV height assignment process: "optimal estimation method using observed radiance and NWP vertical profile". However, it is still to be studied if the small differences between JMA AMVs and the background NWP model used for the processing, imply a good impact in later applications, like NWP assimilation.

Supplementary Materials:

The following supplementary materials are available online:

- amv_dataset.tar.gz: gzipped tar file with all AMV data used in the AMV Intercomparison.
- amv_scripts.tar: tar file with all bash, MATLAB and Python scripts used in the AMV Intercomparison.
- raob.tar.gz: gzipped tar file with the radiosonde data used in the AMV Intercomparison.
- README_Intercomparison.txt: text file describing and explaining how to process the different Supplementary Materials, and how to obtain the "ECMWF ERA-INTERIM reanalysis" used in the AMV Intercomparison.

Author Contributions:

Conceptualization: R. Borde and S. Wanzong; Supervision and funding acquisition: J.García-Pereda; Resources: R.Galante Negri, R.Borde, M.Carranza, K.Nonaka, K.Shimoji, S.M.Oh, B.I.Lee, S.R.Chung, J.Daniels, W.Bresky and J.García-Pereda; Methodology, software, formal analysis and investigation: D.Santek, I.Genkova, R.Dworak, S.Wanzong and S.Nebuda; Writing - Original draft: D.Santek and J.García-Pereda; Writing – Review and editing: D.Santek and J.García-Pereda.

Funding:

The "Space Science and Engineering Center" (SSEC) of "University of Wisconsin-Madison" (UW) was funded to do this research by the "European Organisation for the Exploitation of Meteorological Satellites (EUMETSAT)", through the "Satellite Application Facility on Support to Nowcasting (NWCSAF)" "Visiting Scientist Activity (VSA)" program.

Acknowledgements:

This research has been considered from the general interest by the "International Winds Working Group (IWWG)", to monitor and intercompare the different geostationary AMV algorithms available in the world in a common situation. The IWWG wants to thank colleagues from the "Space Science and Engineering Center" (SSEC) of "University of Wisconsin-Madison" (UW), for the work done with a very tight schedule.

Also, the IWWG thanks:

- The colleagues in the different AMV production centers for the effort to provide the AMV datasets for this AMV Intercomparison: Renato Galante Negri (BRZ), Régis Borde and Manuel Carranza (EUM), Kenichi Nonaka and Kazuki Shimoji (JMA), Soo Min Oh, Byung-Il Lee and Sung-Rae Chung (KMA), Jaime Daniels and Wayne Bresky (NOA) and Javier García-Pereda (NWC).
- Régis Borde and Manuel Carranza (EUM), Kenichi Nonaka and Kazuki Shimoji (JMA), and Wayne Bresky (NOA) for the definition and preparation of the input data for the calculation of the AMVs in the different centers.

Conflicts of Interest:

The whole formal analysis and the investigation was made by researchers completely independent to all AMV algorithms involved in the research.

However, some of the AMV producers participated in the definition and preparation of the common input data for the calculation of the AMVs (R. Borde, M. Carranza, K. Nonaka, K. Shimoji and W. Bresky), and in the supervision and writing of the manuscript (J. García-Pereda). The IWWG and all AMV producers were aware of this and in agreement with these circumstances.

References

1. Menzel, W. P., 2001: Cloud Tracking with Satellite Imagery: From the Pioneering Work of Ted Fujita to the Present. Bull. Amer. Meteor. Soc., Vol. 82, pp. 33-47.
2. Novak, C. and M. Young, 1977: The operational processing of wind estimates from cloud motions: Past, present and future. Proceedings of the 11th International Symposium on Remote Sensing of Environment: Application and processing of remotely sensed data. Ann Arbor, Michigan, United States, April 1977.

3. Bresky, W. C., J. M. Daniels, A. A. Bailey and S. T. Wanzong, 2012: New methods toward minimizing the slow speed bias associated with atmospheric motion vectors. J. Appl. Meteorol. Climatol., Vol. 51, pp. 2137–2151.
4. Smith, E. and D. Phillips, 1972: WINDCO: An interactive system for obtaining accurate cloud motions from geostationary satellite spin scan camera pictures: Measurements from satellite platforms. Scientific Rep. AAS5-115042, Space Science and Engineering Center, University of Wisconsin—Madison, pp. 1–51.
5. Nieman, S., W. L. Smith, C. M. Hayden, D. Gray, S. T. Wanzong, C. S. Velden and J. Daniels, 1997: Fully automated cloud-drift winds in NESDIS operations. Bull. Amer. Meteor. Soc., Vol. 78, pp. 1121-1133.
6. Schmetz, J., K. Holmlund, J. Hoffman, B. Strauss, B. Mason., V. Gaertner, A. Kock and L.V. DeBerg, 1993: Operational cloud-motion winds from Meteosat infrared images. J. Appl. Meteor., Vol. 32, pp. 1206-1225.
7. Borde, R., M. Doutriaux-Boucher, G. Dew, M. Carranza, 2014: A Direct Link between Feature Tracking and Height Assignment of Operational EUMETSAT Atmospheric Motion Vectors. J. Atmos. Oceanic Technol., Vol. 31, pp. 33–46.
8. Kodaira, N., K. Kato and T. Hamada, 1979: Man-machine Interactive Processing of Extracting Cloud Top Height and Cloud Wind Data from GMS Images. Meteorological Satellite Center Technical Note, Vol. 1, pp. 59-78.
9. Machado, L.A.T. and J. Ceballos, 1998: Satellite Based Products for Monitoring Weather in South America: Winds and Trajectories. Proceedings of the 5th International Winds Workshop, Saanenmöser, Switzerland, October 1998.
10. Negri, R. G. and L. A. T. Machado, 2008: CPTEC/INPE Operational GOES-10 Atmospheric Motion Vectors. Proceedings of the 9th International Winds Workshop, Annapolis, Maryland, United States, April 2008.
11. National Institute of Meteorological Sciences (NIMS), 2009: Development of Meteorological Data Processing System for Communication, Ocean and Meteorological Satellite, Vol. 1, pp. 77-101. Available online: http://www.ndsl.kr/ndsl/commons/util/ndslOriginalView.do?dbt=TRKO&cn=TRKO201000010174.
12. García-Pereda, J, 2018: NWCSAF/High Resolution Winds AMV software version 2018. Proceedings of the 14th International Winds Workshop. Jeju, Rep. Korea, April 2018.
13. Genkova, I., R. Borde, J. Schmetz, J. Daniels, C. Velden and K. Holmlund, 2008: Global atmospheric motion vector intercomparison study. Proceedings of the 9th International Winds Workshop, Annapolis, Maryland, United States, April 2008.
14. Genkova, I., R. Borde, J. Schmetz, C. Velden, K. Holmlund, N. Bormann and P. Bauer, 2010: Global atmospheric motion vector intercomparison study. Proceedings of the 10th International Winds Workshop, Tokyo, Japan, February 2010.
15. Santek, D., C. Velden, I. Genkova, S. Wanzong, D. Stettner, M. Mindock and J. García-Pereda, 2014: 2014 AMV Intercomparison Study. Proceedings of the 12th International Winds Workshop, Copenhagen, Denmark, June 2014.
16. Holmlund, K, 1998: The utilisation of statistical properties of satellite derived Atmospheric Motion Vectors to derive Quality Indicators. Weather Forecast., Vol. 13, pp. 1093-1104.
17. Negri, R. G., R. Borde, M. Carranza, K. Nonaka, S.M. Oh, A. Bailey, S. Wanzong and J. García-Pereda, 2018: International Winds Working Group (IWWG) Operational AMV Product Survey. Available online: http://cimss.ssec.wisc.edu/iwwg/Docs/AMVSURVEY2018_TOTAL.pdf.
18. Dee, D.P., S.M. Uppala, A.J. Simmons, P. Berrisford, P. Poli, S. Kobayashi, U. Andrae, M.A. Balmaseda, G. Balsamo, P. Bauer, P. Bechtold, A.C.M. Beljaars, L. van de Berg, J. Bidlot, N. Bormann, C. Delsol, R. Dragani, M. Fuentes, A.J. Geer, L. Haimberger, S.B. Healy, H. Hersbach, E.V. Hólm, L. Isaksen, P. Kållberg, M. Köhler, M. Matricardi, A.P. McNally, B.M. Monge-Sanz, J.-J. Morcrette, B.-K. Park, C. Peubey, P. de Rosnay, C. Tavolato, J-N. Thépaut and F. Vitart, 2011: The ERA-Interim reanalysis: configuration and performance of the data assimilation system. Q.J.R.Meteorol.Soc., Vol. 137, pp. 553–597.
19. Salonen, K., J. Cotton, N. Bormann and M. Forsythe, 2012: Characterising AMV height assignment error by comparing best fit pressure statistics from the Met Office and ECMWF system. Proceedings of the 11th International Winds Workshop, Auckland, New Zealand, February 2012.